Wideband BPF for 5G mm-wave Applications with Detailed Extraction of Poles and Zeros

Aqeela Saghir, Salman Arain, Abdul Quddious, Symeon Nikolaou, and Photos Vryonides
Frederick Research Center,
Frederick University
Nicosia, Cyprus
aqeela.saghir1@seecs.edu.pk, engr.salman16@gmail.com, 12mseeaquddious@seecs.edu.pk, s.nikolaou@frederick.ac.cy, eng.vp@frederick.ac.cy

***Abstract*— A simple design structure for a wideband bandpass filter (BPF) for 5G mm-wave applications is presented in this paper. Sharp skirt with good isolation level is demonstrated by using three pairs of parallel coupled lines (PCLs) and two open-ended stubs. A thorough mathematical derivation by adopting the even- and odd analysis is performed. The simulated and calculated results are in good agreement thus validating the proposed design.**

Keywords—bandpass filter; transmission poles and zeros.

I. INTRODUCTION

High quality bandpass filters (BPFs) have been a key factor for tens of wireless communications front-ends' applications. To name a few, autonomous cars with car-to car connectivity, IoT/IoE mobile and satellite communication transceivers require one or more bandpass filter. These technological need have led to major advancements in electronics and microwaves including the specialized area dealing with multi-band and multi-standard at mm-wave communications. Since 5G wireless systems will utilize mm-wave frequencies (24.5-29.5 GHz) in order to facilitate wide bandwidth and therefore faster data rates, to large-area distributed users, high-performance mm-wave bandpass filters will be greatly required. Especially for small-cell front-end modules where isolation on frequency bands from nearby interference is essential [1]-[4].

This paper demonstrates a novel, simple design structure of a wideband bandpass filter with central frequency of 27 GHz and fractional bandwidth (FBW) of 22% for 5G mm-wave applications. In addition, the extraction methodology of the transmission poles and zeros is carried out analytically based on the even- and odd analysis. A detailed design procedure with mathematical analysis is demonstrated firstly, followed by behaviour confirming simulation results.

II. FILTER DESIGN

The proposed configuration is illustrated in Fig. 1. It consists of three pairs of parallel coupled lines PCLs and two open-ended stubs with characteristic impedances Z_{e1}, Z_{o1}, Z_{e2}, Z_{o2}, Z_{e3}, Z_{o3} and Z_s respectively. The open-ended stubs are placed between the second and third PCLs whereas the ports are connected between the first and second ones. All transmission lines have the same electrical length, θ. To analytically calculate the positions of the transmission poles and zeros the even- and odd analysis is adopted where the original circuit is simplified into even- and odd equivalent

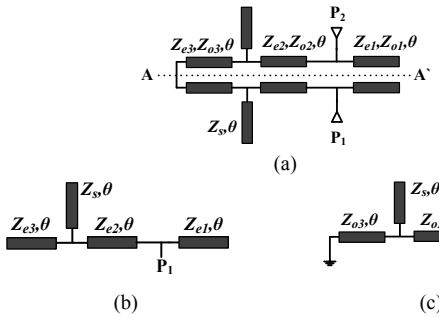

Fig. 1. (a) Proposed mm-wave BPF, (b) Even-mode equivalent circuit, (c) Odd-mode equivalent circuit.

circuits as shown in Fig. 1(a) and Fig. 1(b) respectively. The corresponding even- and odd admittances are given in (1) and (2). The positions of the transmission poles are found when (3) is set to zero [5].

$$Y_{ine} = j\frac{-y_3 \tan^3\theta + y_1 \tan\theta}{-y_2 \tan^2\theta + y_0} \tag{1}$$

$$Y_{ino} = j\frac{x_4 \tan^4\theta - x_2 \tan^2\theta + x_0}{-x_3 \tan^3\theta + x_1 \tan\theta} \tag{2}$$

$$Y_{ine}Y_{ino} - {Y_0}^2 = 0 \tag{3}$$

By inserting (1) and (2) in (3) and simplifying, the following equation is obtained:

$$\begin{aligned} &-x_4y_3 \tan^6\theta + \tan^4\theta(x_2y_3 + x_4y_1 - x_3y_2) + \\ &\tan^2\theta(x_1y_2 + x_3y_0 - x_0y_3 - x_2y_1) + x_0y_1 - x_1y_0 = 0 \end{aligned} \tag{4}$$

Where ,

$$y_0 = Z_{e1}Z_{e2}Z_{e3}Z_s \tag{5}$$

$$y_1 = Z_{e1}Z_{e2}Z_s + Z_{e1}Z_{e2}Z_{e3} + Z_{e1}Z_{e3}Z_s + Z_{e2}Z_{e3}Z_s \tag{6}$$

$$y_2 = Z_{e1}{Z_{e2}}^2Z_s + Z_{e1}{Z_{e2}}^2Z_{e3} \tag{7}$$

$$y_3 = {Z_{e2}}^2Z_s + {Z_{e2}}^2Z_{e3} \tag{8}$$

$$x_0 = Z_{o1}Z_{o2}Z_s \tag{9}$$

$$x_1 = Z_{o1}Z_{o2}Z_{o3}Z_s + Z_{o1}{Z_{o2}}^2Z_s \tag{10}$$

$$x_2 = Z_{o1}Z_{o2}Z_{o3} + Z_{o1}Z_{o3}Z_s + Z_{o2}Z_{o3}Z_s + {Z_{o2}}^2 Z_s \quad (11)$$

$$x_3 = Z_{o1}{Z_{o2}}^2 Z_{o3} \quad (12)$$

$$x_4 = {Z_{o2}}^2 Z_{o3} \quad (13)$$

By solving (4) and considering only the real solutions, three transmission poles are obtained and are shown in Table I.

A similar derivation of the transmission poles is followed for the transmission zeros. To predict the positions of the transmission zeros (14) is set to zero.

$$Y_{ine} - Y_{ino} = 0 \quad (14)$$

Again, by inserting (1) and (2) into (14) the following equation for the transmission zeros is obtained:

$$m_6 \tan^6\theta + m_4 \tan^4\theta + m_2 \tan^2\theta + m_0 = 0 \quad (15)$$

Where,

$$m_6 = Z_{e2}^2 Z_{o2}^2 \left(Z_{e1}Z_{o3}\left(Z_s + Z_{e3}\right) - Z_{o1}Z_{o3}\left(Z_s - Z_{e3}\right)\right) \quad (16)$$

$$m_4 = Z_s \left[\begin{array}{l} Z_{e2}Z_{o2}^2 Z_{o3}\left(\begin{array}{l} Z_{e3}Z_{o1}\left(1+Z_{e1}\right) \\ +Z_{e1}\left(Z_{o1} - Z_{e3}\right) \end{array} \right) \\ Z_{e2}^2 \left(Z_{e1}\left(\begin{array}{l} Z_{o2}^2\left(Z_s - Z_{e3}\right) - Z_{o1}Z_{o3}\left(Z_{o2} + Z_s + Z_{e3}\right) \\ -Z_{o2}Z_{o3}\left(Z_s + Z_{e3}\right) \end{array} \right) \right. \\ \left. +Z_{o1}Z_{o2}\left(Z_{o3}Z_s + Z_{e3}^2 + Z_{e3}Z_{o1}\right) \right) \\ + Z_{e1}Z_{e3}Z_{o1}Z_{o2}^2 Z_{o3} + Z_{e1}Z_{e2}^2 Z_{e3}Z_{o1}Z_{o2}Z_{o3} \end{array} \right] \quad (17)$$

$$m_2 = Z_s^2 \left[\begin{array}{l} Z_{e2}\left(\begin{array}{l} Z_{e1}Z_{e3}\left(Z_{o3}\left(Z_{o1} + Z_{o2}\right) + Z_{o2}^2\right) \\ +Z_{o1}Z_{o2}\left(\begin{array}{l} Z_{e1}\left(Z_{e2} - Z_{o2} - Z_{o3}\right) \\ -Z_{e3}\left(Z_{o1} + Z_{o2}\right) \end{array} \right) \end{array} \right) \\ -Z_{e1}Z_{e3}Z_{o1}Z_{o2}\left(Z_{o2} + Z_{o3}\right) \\ + Z_s Z_{e1}Z_{e2}Z_{e3}Z_{o1}Z_{o2}\left(Z_{e2} - Z_{o2}\right) \end{array} \right] \quad (18)$$

$$m_o = Z_{e1}Z_{e2}Z_{e3}Z_{o1}Z_{o2}Z_s^2 \quad (19)$$

Again, considering only the real solutions of (15) four transmission zeros are obtained and are tabulated in Table I.

III. Simulation Results

The proposed filter is simulated on a substrate with relative dielectric constant ε_r=3.55 and thickness h=0.813 mm. The layout of the proposed design with the dimensions is depicted in Fig. 2. To verify the theoretical calculations, full-wave simulation is carried out with the results depicted in Fig. 3. The corresponding impedances are Z_{e1}=154Ω, Z_{e2}=139Ω, Z_{e3}=124Ω, Z_{o1}=95Ω, Z_{o2}=87Ω, Z_{o3}=124Ω, Z_s=70Ω. The electrical length of all transmission lines θ is at 90° at the operating frequency of 27 GHz. It can be clearly seen from Fig. 2 that three transmission poles and four transmission zeros are observed. All simulated and calculated poles and zeros are listed in Table I. From Table I it can be said that calculated and simulated results are almost identical thus validating the mathematical equations.

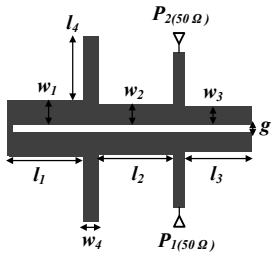

Fig. 2. Proposed design layout with dimensions (units in mm) (l_1=1.7, l_2=1.7, l_3=1.7, l_4=1.7, w_1=0.47, w_2=0.35, w_3=0.25, w_4=1.15, g= 0.2.

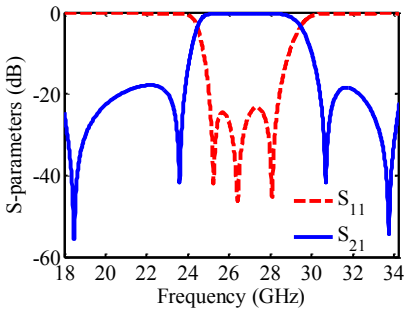

Fig. 3. Simulated S-parameters results of the proposed mm-wave BPF.

TABLE I
THEORETICAL AND SIMULATED POSITIONS OF POLES AND ZEROS (UNITS:GHZ)

	Transmission Poles		Transmission Zeros	
	Theoretical	Simulated	Theoretical	Simulated
1	25.19	25.24	18.34	18.48
2	26.38	26.41	23.45	23.60
3	27.96	28.08	30.52	30.68
4	-	-	33.65	33.74

IV. Conclusions

In this paper a wideband BPF for 5G mm-wave applications is demonstrated. The analysis of this filter is concentrated on accurately predicting the transmission poles and zeros by deriving the circuit equations. Simulations agree well with the calculated values.

Acknowledgment

This research was partially funded from Cyprus' RPF, RESTART2016-2020 EXCELLENCE/1216/376.

References

[1] M. Ali *et al*., "First Demonstration of Compact, Ultra-Thin Low-Pass and Bandpass Filters for 5G Small-Cell Applications," in *IEEE Microwave and Wireless Components Letters*, vol. 28, no. 12, pp. 1110-1112, Dec. 2018.

[2] M. Ali *et al*., "Miniaturized High-Performance Filters for 5G Small-Cell Applications," *2018 IEEE 68th Electronic Components and Technology Conference (ECTC)*, San Diego, CA, 2018, pp. 1068-1075.

[3] K. Y. Chan, R. Ramer, R. R. Mansour and Y. J. Guo, "60 GHz to E-Band Switchable Bandpass Filter," in *IEEE Microwave and Wireless Components Letters*, vol. 24, no. 8, pp. 545-547, Aug. 2014.

[4] K. Y. E. Chan, R. Ramer and Y. J. Guo, "RF MEMS millimeter-wave switchable bandpass filter," *2013 IEEE International Wireless Symposium (IWS)*, Beijing, 2013, pp. 1-4.

[5] J. Hong and M.J. Lancaster, Microstrip filters for RF/microwave applications. New Yok: Wiley 2001.